Unoccupied electronic structure of Ru(0001)

W.-K. Siu* and R. A. Bartynski
Department of Physics and Astronomy and Laboratory for Surface Modification, Rutgers University, 136 Frelinghuysen Road, Piscataway, New Jersey 08854, USA

(Received 26 February 2007; revised manuscript received 4 May 2007; published 19 June 2007)

The unoccupied electronic states of the clean Ru(0001) surface were measured along the $\bar{\Gamma}\,\bar{K}$ and $\bar{\Gamma}\,\bar{M}$ high symmetry axes of the surface Brillouin zone (SBZ) using angle-resolved inverse photoemission spectroscopy. The spectra are dominated by strong emission within the first 2 eV above the Fermi level and, but for a weak image potential state, are essentially featureless at higher energies (up to ~6 eV). The spectra obtained along the $\bar{\Gamma}\,\bar{K}$ direction exhibit three well-defined features that are identified as originating from bulk direct transitions. The dispersions with parallel momentum for two of the three features run along the edges of projected band gaps found in *ab initio* electronic structure calculations. Detailed examination of these spectra reveals the presence of a surface state that appears near $k_{\|}=0.7$ Å and persists to the boundary of the SBZ. The spectra along the $\bar{\Gamma}\,\bar{M}$ direction exhibit less well-defined features, but comparing spectra from the clean surface to those obtained from a surface exposed to 0.5 L (1 L$=10^{-6}$ Torr s) of CO enables identification of four additional peaks arising from bulk direct transitions. One feature may be associated with a surface resonance that is predicted to exist near the $\bar{M}$ point. Comparison of the observed dispersions with those predicted for states along the high symmetry directions of the bulk gives a good account of the experimental data.

DOI: 10.1103/PhysRevB.75.235427 PACS number(s): 73.20.−r, 71.20.Be, 79.60.−i, 79.20.Kz

I. INTRODUCTION

The electronic structure of ruthenium (Ru) has been studied for decades because of its application in catalytic processes, such as methanation.[1–3] Knowledge of the bulk and surface electronic structure of Ru is essential in understanding the behavior of the clean and adsorbate covered Ru surfaces. For the clean Ru surface, several theoretical studies of the electronic band structure have been performed.[4–7] In addition, there has been ongoing interest in experimental studies of the occupied electronic states of clean Ru for many years.[8–11] However, there has not been extensive examination of the unoccupied electronic states of Ru. In contrast, the study of the adsorption of gases on Ru is more diverse and wide ranging as compared to clean Ru surface studies. Gases commonly used in adsorption studies are CO,[12–19] NO,[20–22] H_2,[23–25] and some other simple gases.[26–30] The adsorption of CO on the clean and alkali-metal-promoted Ru(0001) surfaces has received seemingly continuous experimental interest.[19,26,27,30–34] Coadsorption studies have focused on CO with oxygen[27,30] and the effect of the presence of alkali metal on the Ru(0001) surface.[32,34] Owing to the importance of alkali metals in influencing catalytic activity, the study of CO on alkali-metal-promoted Ru surfaces has also received considerable attention.[35–38] Various properties of CO on clean Ru(0001) have been investigated, including the binding energy of CO,[31] the bonding sites,[26] and the geometry of CO on the Ru(0001) surface.[19] Recently, there has been considerable interest in the unusual behavior of water upon adsorption on the Ru(0001) surface.[39–46]

Most studies of the clean Ru surface have focused on the high symmetry (0001) orientation because it has the lowest surface free energy and thus is most likely to be exposed in practical applications. Theoretical studies of the clean Ru(0001) electronic band structure have been done by several authors.[5,6] There are only a few experimental measurements of the unoccupied electronic states of the clean Ru(0001) surface.[9,18,47] Furthermore, most of those measurements focus on normal incidence, examining the Γ-A direction of the bulk Brillouin zone. The unoccupied states within a few eV of the Fermi level are the most interesting because they have the greatest influence on the chemical properties of the surface. In this paper, we report measurements of the unoccupied states along the high symmetry directions of the Ru(0001) surface using inverse photoemission spectroscopy (IPES). In a recent experiment using angle-resolved ultraviolet photoemission spectroscopy (ARUPS), the occupied electronic states of the Ru(0001) surface have been mapped.[11] Our study is highly complementary to the information provided in that work.

The remainder of this paper is organized as follows. The experimental setup used for the IPES measurements is described in Sec. II. A brief review of the crystallographic structure of Ru is presented in Sec. III, while the results of our IPES measurements of the Ru(0001) surface along the $\bar{\Gamma}\,\bar{K}$ and the $\bar{\Gamma}\,\bar{M}$ high symmetry directions are discussed in Secs. IV and V, respectively. To obtain a better understanding of the features characteristic of the clean Ru(0001) surface, IPES measurements from a slightly CO-covered, e.g., 0.5 L (1 L$=10^{-6}$ Torr s), Ru(0001) surface are compared to those from the clean Ru(0001) surface. Section VI discusses and compares the experimental results with theoretical calculations. In Sec. VII, we summarize our findings and conclusions.

II. EXPERIMENTAL ASPECTS

Experimental measurements were carried out in an ultrahigh vacuum (UHV) chamber attached to an IPE grating spectrograph that has been described in earlier publications.[48,49] Briefly, the experimental chamber houses a

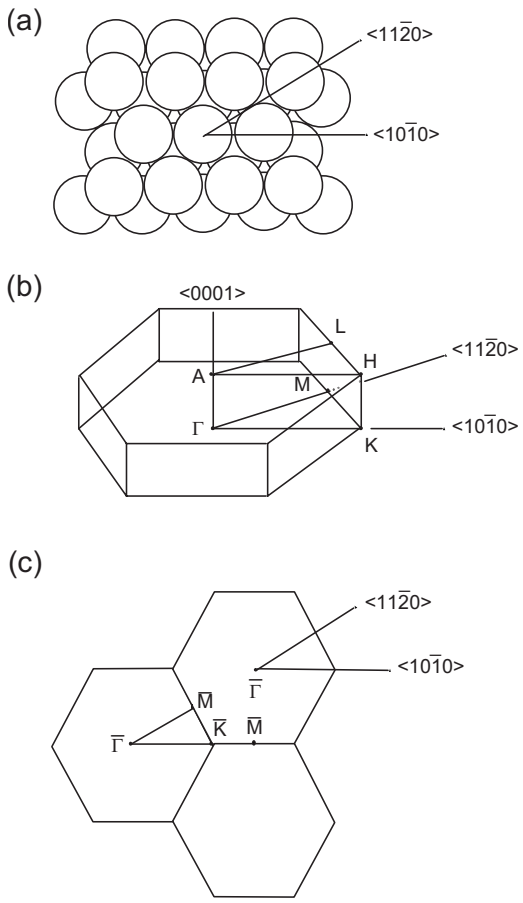

FIG. 1. Ru crystal structure in real and reciprocal spaces: (a) the Ru(0001) surface in real space, (b) the first Brillouin zone of Ru, and (c) the surface Brillouin zone (SBZ) of the Ru(0001) surface with the critical points $\bar{\Gamma}$, $\bar{K}$, and $\bar{M}$ labeled.

low energy electron diffraction apparatus, an IPE electron gun, a leak valve for controlled introduction of gases, and the sample which is mounted on a two-axis goniometer. The base pressure of the UHV chamber is 1×10^{-10} Torr (1.33×10^{-8} Pa). The electron gun produces a well collimated beam ($\Delta\theta\leqslant0.5°$) at a fixed electron energy, typically between 12 and 25 eV. Photons emitted from the sample during the IPE process are collected and dispersed by a concave spherical diffraction grating and projected onto a position sensitive detector. The sample, grating, and detector are mounted on the Rowland circle. One axis of the detector is aligned with the dispersion direction of the grating so that the position of an event on the detector corresponds to the energy of the emitted photon. IPE spectra are acquired by recording the number of photons detected as a function of photon energy for a fixed incident electron energy. The overall energy resolution, including the electronic resolution and the optical arrangement of IPE spectrograph, is ~0.3 eV.

The substrate was a Ru single crystal disk of ~2 mm thickness with its surface aligned along the (0001) orientation. The crystal was mechanically polished down to a grit size of 0.25 μm and the orientation was within 0.5° of the desired high symmetry orientation. The crystal was spot-welded to, and supported by, a pair of Ta wires. A C-type

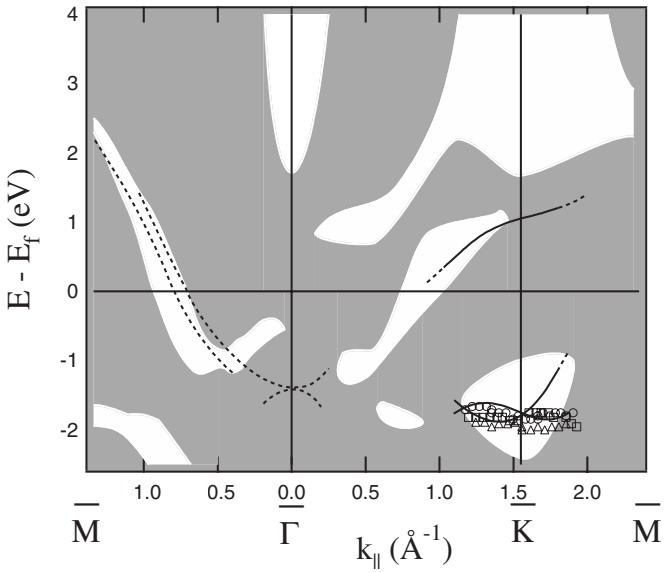

FIG. 2. Projected band structure of Ru(0001) by Holzwarth and Chelikowsky (Ref. 6). The shaded regions indicate the projected bulk states. The dotted lines are surface resonances and the solid lines indicate surface states. Plotted in the lower right corner are the photoemission data of the surface states of Ru(0001) as measured by Pelzer *et al.* (Ref. 11).

thermocouple (W-5%Re/W-26%Re) was attached to the rim of the sample. The sample was initially cleaned by sputtering with 1 keV Ar^+ ions and repeated cycles of annealing (~1100 K) in oxygen at 1×10^{-6} Torr to remove carbon, the main contaminant of this material.[47,50] After several cleaning cycles, the sample was flashed to a temperature of ~1800 K for 1 min via electron beam heating. The IPE spectrum shows a well-developed image potential state indicating that a clean surface resulted from the high temperature flashing. The IPE spectra were acquired at room temperature.

The Ru(0001) crystal could be rotated azimuthally about the ⟨0001⟩ surface normal. In addition, the manipulator is able to rotate about a second axis which is perpendicular to the sample normal and lies in the plane of the crystal surface. For the experiments discussed here, the Ru crystal was oriented such that either the $\bar{\Gamma}\,\bar{K}$ (⟨10$\bar{1}$0⟩) or the $\bar{\Gamma}\,\bar{M}$ (⟨11$\bar{2}$0⟩) directions of the surface could be scanned by the IPES electron gun when the second axis is rotated.

To assist in distinguishing between surface and bulk-derived features, IPE spectra from the clean surface were occasionally compared to spectra acquired from a sample after exposure to small amounts (~0.5 L) of CO. The CO-covered Ru(0001) surface was prepared by back filling the chamber with CO to a pressure of 1×10^{-8} Torr.

III. SURFACE GEOMETRIC STRUCTURE OF Ru

Ru has an hcp crystal structure. The Ru atoms arrange in a hexagonal array for each layer in the unit cell. The layers are stacked in an *ABAB*… sequence. The arrangement of atoms on the Ru(0001) surface is shown in Fig. 1(a). The in-plane and out-of-plane lattice constants of Ru are *a*

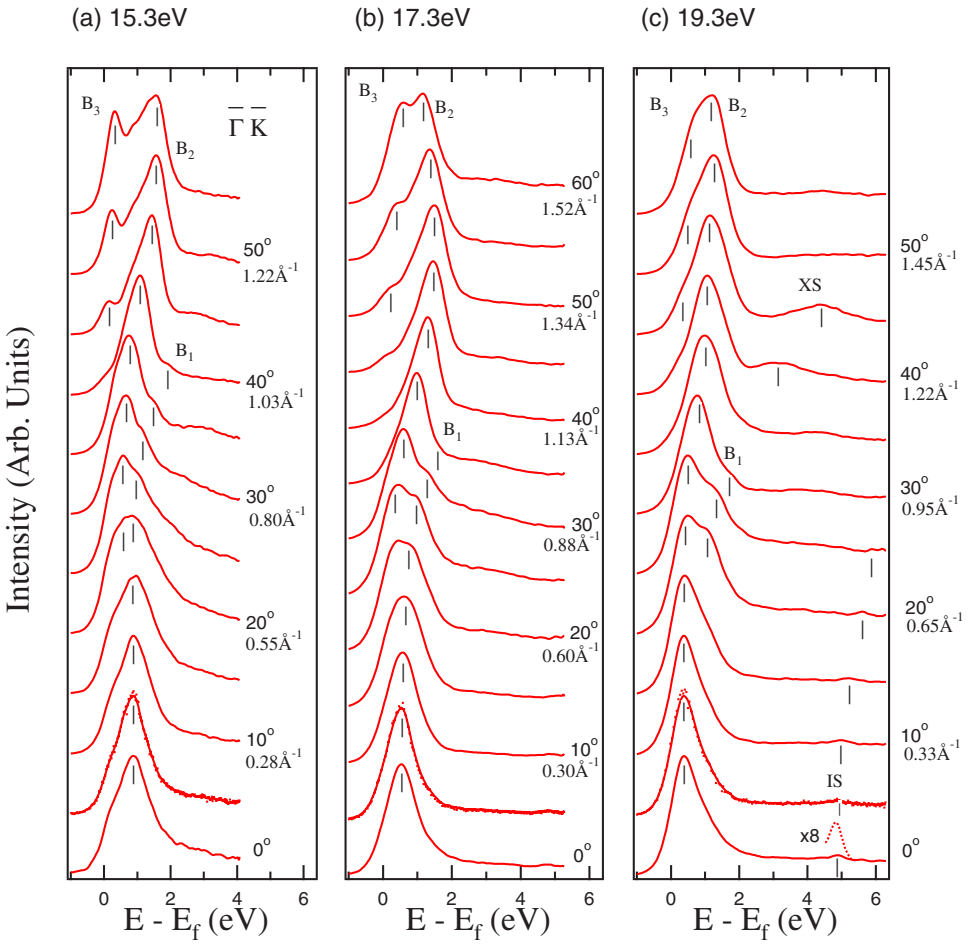

FIG. 3. (Color online) IPE spectra of the clean Ru(0001) surface along the $\bar{\Gamma}\,\bar{K}$ direction. The incident electron energies, $E_i - E_F$, are (a) 15.3 eV, (b) 17.3 eV, and (c) 19.3 eV. The image potential state (IS) and the bulk transitions B_1, B_2, and B_3 are indicated by tick marks.

=2.704 Å and c=4.282 Å, respectively, and the work function of Ru(0001) surface is 5.52 eV.[51] The bulk Brillouin zone of Ru is shown in Fig. 1(b). The high symmetry directions in the Brillouin zone are shown in the figure.

The hcp (0001) surface Brillouin zone (SBZ) is shown in Fig. 1(c), as a projection of the bulk Brillouin zone along the $\langle 0001 \rangle$ direction. The critical points are labeled as $\bar{\Gamma}$, $\bar{K}$, and $\bar{M}$ in the SBZ of the (0001) surface. The crystallographic directions and the sizes of $\bar{\Gamma}\,\bar{K}$ and $\bar{\Gamma}\,\bar{M}$ are $\langle 10\bar{1}0 \rangle$, 1.55 Å^{-1} and $\langle 11\bar{2}0 \rangle$, 1.34 Å^{-1}, respectively. Extension of the SBZ beyond the first zone along the $\bar{\Gamma}\,\bar{M}$ direction is the mirror of $\bar{\Gamma}\,\bar{M}$, that is, $\bar{M}\,\bar{\Gamma}$. The extension along the $\bar{\Gamma}\,\bar{K}$ direction, however, does not encounter the reverse of $\bar{\Gamma}\,\bar{K}$, but the $\bar{K}\,\bar{M}$ direction, that is, $\bar{\Gamma}\,\bar{K}\,\bar{M}$ in a straight line. This property makes the IPES measurement along the $\bar{\Gamma}\,\bar{K}$ direction more interesting since after crossing the $\bar{K}$ point, one can probe the $\bar{K}\,\bar{M}$ line, a portion of the SBZ that is otherwise difficult to access.

For IPES, the perpendicular momentum $\boldsymbol{k}_\perp$ of the incident electron is not conserved upon interaction with the crystal surface. Only the parallel momentum $\boldsymbol{k}_\parallel$ of the incident electron is conserved upon interaction with the crystal surface. The magnitude of $\boldsymbol{k}_\parallel$ is given by the expression $k_\parallel = \sqrt{\frac{2m_e}{\hbar^2}}(E_i - \Phi)\sin\theta$, where E_i is the energy of incident electron above the Fermi level of the Ru(0001) surface, Φ is the work function of the Ru(0001) surface, which is 5.52 eV,[51] and θ is the incident angle of the electron with respect to the normal of the Ru(0001) surface.

Figure 2 shows the results of a theoretical calculation of the projected electronic band structure of the Ru(0001) surface by Holzwarth and Chelikowsky.[6] The shaded area is the projected bulk states. The dotted lines are predicted surface resonances and the solid lines are surface states. The results of an ARUPS study of occupied surface states near the $\bar{K}$ point of Ru(0001) performed by Pelzer *et al.*[11] are plotted in the lower right corner of Fig. 2. The photon energies used in those ARUPS ranged from 35 to 45 eV. The energy and dispersion of the UPS data agree with those predicted for the Ru(0001) surface states. IPES provides information that is complementary to these UPS measurements in that it probes the unoccupied electronic band structure of Ru(0001) above the Fermi level. In the calculations presented in Fig. 2, only one unoccupied surface state is predicted and its dispersion extends from mid-$\bar{\Gamma}\,\bar{K}$ past $\bar{K}$ to the mid-$\bar{K}\,\bar{M}$ range. Two surface resonances are also predicted, and they extend from ~1.5 eV below the Fermi level at $\bar{\Gamma}$ to ~2 eV above the Fermi level at $\bar{M}$.

IV. UNOCCUPIED ELECTRONIC STATES OF Ru ALONG THE $\bar{\Gamma}\,\bar{K}$ DIRECTION

Angle-resolved IPE spectra on Ru(0001) were acquired along the $\bar{\Gamma}\,\bar{K}$ direction at angles of incidence from 0° (i.e.,

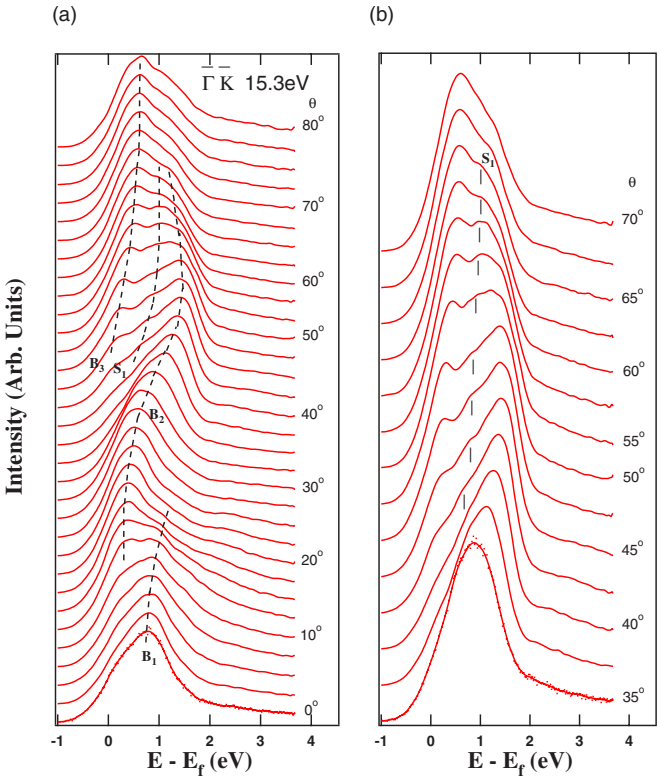

FIG. 4. (Color online) (a) IPE spectra of the Ru(0001) surface along the $\bar{\Gamma}\,\bar{K}$ direction at incident energy of 15.3 eV in angular steps of 2.5° from 0° to 80°. The bulk state transitions are labeled as B_1, B_2, and B_3. The surface states are labeled as S_1. (b) The IPE spectra between 35° to 70° are displaced for illustrating surface state S_1 in (a). The tick marks are the positions of surface state S_1.

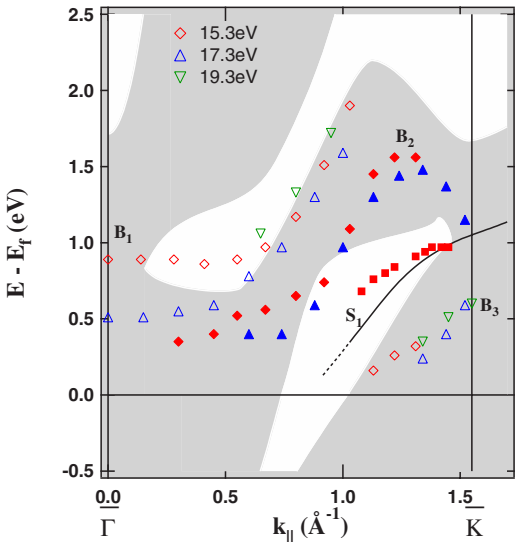

FIG. 5. (Color online) The dispersion of features observed in the IPE spectra from Ru(0001) along the $\bar{\Gamma}\,\bar{K}$ direction. Bulk states B_1, B_2, and B_3 and surface states S_1 along the $\bar{\Gamma}\,\bar{K}$ direction of the Ru(0001) surface are indicated by symbols. The diamond, upward triangle, and downward triangle represent the incident energies at 15.3, 17.3, and 19.3 eV, respectively.

normal incidence) to 55° at 5° steps. The incident electron energies for the spectra, shown in Figs. 3(a)–3(c), were 15.3, 17.3, and 19.3 eV above the Fermi level of the Ru(0001) surface, respectively. In each figure, the θ=5° spectrum shows the raw data points illustrating that the noise level is comparable to the thickness of the lines, which are digital smooths to the data. The parallel momentum of each spectrum $k_\parallel$ is shown next to the angle. The IPES spectra show a similar behavior for all three incident energies as a function of incident angle. The energy range of the spectra is larger for a higher incident energy owing to the photon energy dispersion of the IPES spectrograph used in these experiments. As $k_\parallel$ is a function of incident electron energy, the parallel momentum increases with increasing electron energy even at the same incident electron angle.

Basically, the IPES spectra could be identified as having three main features, labeled as B_1, B_2, and B_3. At normal incidence, the feature labeled B_1 has a well-defined peak at ~1 eV above the Fermi level and does not appear to disperse with increasing incident angle until ~20°. For larger angles, state B_1 shows a rapid dispersion with the incident angles away from E_F and diminishes in intensity at $k_\parallel \sim 1.0$ Å^{-1} where it has reached an energy of about 2 eV above the Fermi level.

Feature B_2 appears as a subtle shoulder on the low energy side of B_1 at small angles in the data obtained at 15.3 eV, but is not clearly visible in these IPE spectra until $k_\parallel$ is increased to ~0.5 Å^{-1}. It appears to come from below E_F with increasing angle, but it is hard to locate the incident angle at which state B_2 crosses the Fermi level. In these spectra, the feature is not clearly resolved until it is ~0.3 eV above the Fermi level. State B_2 has a rapid dispersion with the incident angles and moves in an energy range from ~0.2 to ~2 eV. In the spectra obtained at 17.3 eV [see Fig. 3(b)], the state clearly exhibits a dispersion with incident angle that shows a bending to a lower energy when passing $k_\parallel$=1.34 Å^{-1}. This is also present in the 19.3 eV spectra, but is not as pronounced because the larger values of $k_\parallel$ were not probed. The distinction between states B_1 and B_2 for θ<20° in the spectra taken at 19.3 eV is difficult to observe.

A sharp state B_3 emerges from the Fermi level at $k_\parallel$ about 1.1 Å^{-1} in the spectra obtained at 15.3 eV. From Fig. 3, the intensity of B_3 shows a strong dependence on the incident energy, decreasing rapidly as the incident energy increases.

Finally, we note that in the spectra obtained at 19.3 eV, the image potential state (IS), which is the first state of Rydberg-like series of unoccupied states bound close to the vacuum level by the image potential of an electron, is observed at 5.0±0.2 eV above the Fermi level. The energy of IS is consistent with the work function of Ru(0001) which is 5.5 eV. The state IS exhibits a parabolic dispersion with $k_\parallel$ demonstrating free-electron-like behavior in the plane of the surface. As IS overlaps the inelastic background of the strong features near the Fermi level, its relative intensity is comparatively weak.

The lack of features (other than the image state) in the normal incidence spectra at energies greater than 2 eV above E_F is consistent with the band structure calculation in Fig. 2. There is a projected band gap of Ru(0001) at $\bar{\Gamma}$ in the energy range above 2 eV. Another projected band gap is predicted

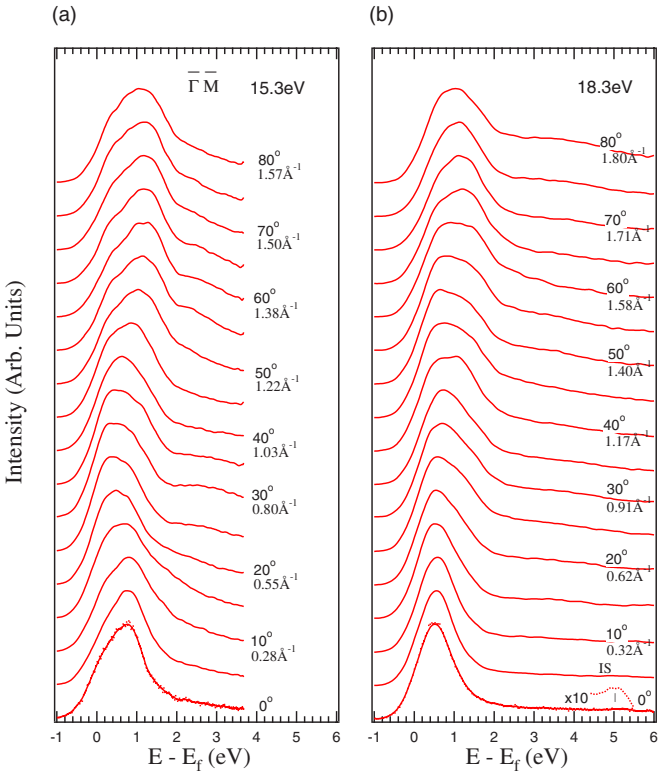

FIG. 6. (Color online) IPE spectra of the clean Ru(0001) surface along the $\bar{\Gamma}\,\bar{M}$ direction measured with incident energies of (a) 15.3 eV and (b) 18.3 eV.

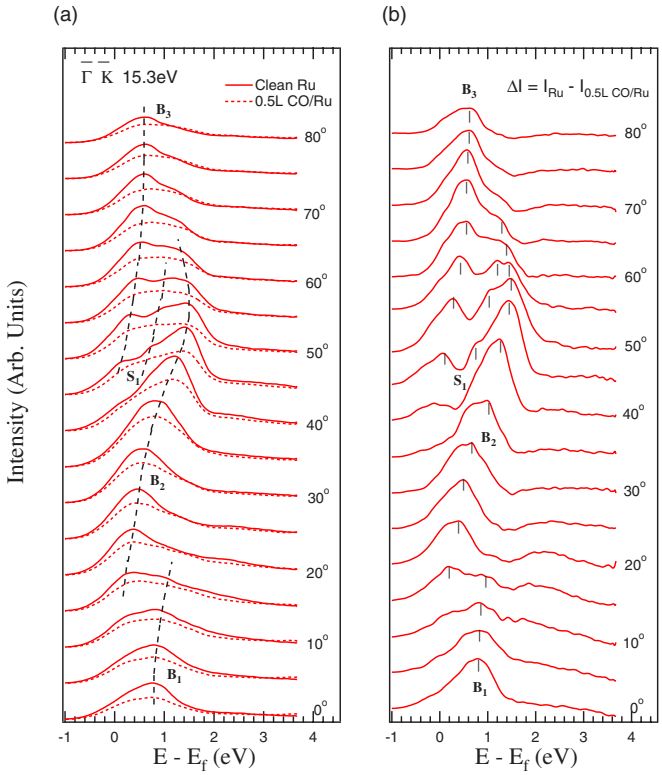

FIG. 7. (Color online) Illustration of difference spectra from the Ru(0001) surface. (a) The tick marks indicate features S_1, B_2, and B_3. The IPE spectra from the clean Ru surface (solid lines) and the spectra from 0.5 L CO-exposed Ru surface (dashed lines) were measured along the $\bar{\Gamma}\,\bar{K}$ direction at 15.3 eV above the Fermi level. (b) The difference spectra reveal clear, well-resolved features indicated by tick marks.

around $\bar{K}$ for energies greater than 2 eV. In Fig. 3(c), a feature is observed in the spectra taken at 19.3 eV around 1.22 $Å^{-1}$ (θ=40°) which is labeled as XS. This feature is in the region of the projected band gap near $\bar{K}$. The unknown feature XS may be another surface state that has not been predicted.

The spectra in Fig. 3 show a wide range of angles obtained at relatively coarse angular steps (5° each) to cover three incident energies. In order to probe the unoccupied states in more detail, Fig. 4(a) shows IPE spectra measured at an incident energy of 15.3 eV spanning angles from 0° to 80° in 2.5° steps. As compared to the spectra in Fig. 3, states B_1, B_2, and B_3 are more easily observed and show the same energy dispersion with the incident angles. The dotted lines are guides for the eye that indicate the dispersions of these states. Compared to Fig. 3, state B_2 shows a clear dispersion bending at around 45° and state B_3 crosses the Fermi level at $\theta \sim 47°$.

A closer examination of the result in Fig. 4(a) shows a weak signal, labeled S_1, visible in the angular range from 42.5° to 65° at the energy about 0.6–0.8 eV which is not easily observed in Fig. 3. These key IPE spectra from Fig. 4(a) are magnified and displayed in Fig. 4(b). The tick marks indicate the weak state S_1, which shows a small dispersion with the incident angles, $k_\parallel$. The weak intensity of state S_1 may be a sign of a high sensitivity to surface contamination or a low cross section. Also, state S_1 is between two strong states, B_2 and B_3, making it even more difficult to detect its presence.

Figure 5 shows the dispersion with $k_\parallel$ along $\bar{\Gamma}\,\bar{K}$ of the features identified in Figs. 3 and 4. The shaded area is the projected bulk band of Ru(0001) from Fig. 2. The shapes of the symbols (diamond, upward triangle, and downward triangle) represent the incident energies 15.3, 17.3, and 19.3 eV, respectively. Data for B_2 in the range of $k_\parallel < 0.5$ are taken from the spectra of Fig. 4. State S_1 in Fig. 4 is also plotted in Fig. 5.

In Fig. 5, state B_1 has a flat dispersion with $k_\parallel$ around $\bar{\Gamma}$ and follows the edge of the projected band structure. The difference in energies of state B_1 in the spectra taken at 15.3 eV and those taken at 17.3 eV is due to the incident electrons coupling to different energy initial unoccupied states which have different perpendicular momenta in the ΓA direction of the bulk Brillouin zone. Upon a direct radiative transition, electrons with different incident energies access slightly different energies in the final band. State B_2 shows a rapid upward dispersion with $k_\parallel$ and then bends downward near $k_\parallel$=1.2 $Å^{-1}$, following the shape of the upper edge of the project band structure. The dispersion of B_3 is monotonically increasing with $k_\parallel$. States B_1, B_2, and B_3 are in the projected bands of Ru(0001) where B_1 and B_2 appear to follow the projected band edge dispersion. Hence, it is strongly suggested that they originate from Ru bulk transitions.

State S_1 is in the projected band gap of Ru(0001) from 1.0 to 1.4 $Å^{-1}$. The experimental results are close to the solid

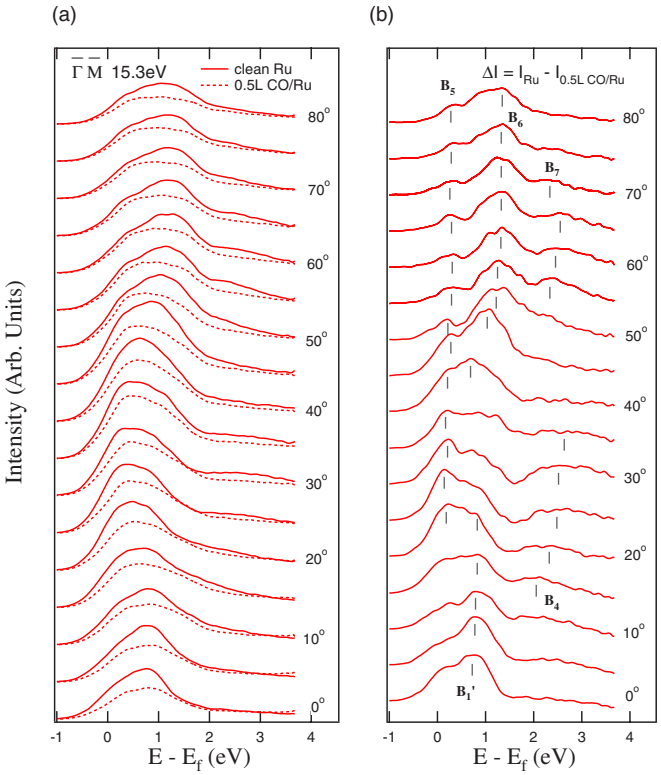

FIG. 8. (Color online) (a) IPE spectra of the clean and 0.5 L CO-covered Ru(0001) surface along the $\bar{\Gamma}\,\bar{M}$ direction at an incident energy of 15.3 eV. (b) The difference spectra of the clean Ru(0001) IPE spectra to the spectra of CO-covered Ru(0001) surface in (a). The enhanced features in the Ru(0001) surface are indicated by tick marks.

line, which is the predicted surface state along the $\bar{\Gamma}\,\bar{K}$ direction. The dotted portion of this line is the predicted surface resonance, which is not observed in our IPE spectra. The surface resonance may have weaker emission or a weaker interaction with the incident electron. Also, if it exists, it is difficult to distinguish from states B_2 and B_3 near $\bar{K}$ as all three features are within 0.5 eV of each other. The experimental data of state S_1 are close to the calculated surface state, being ~0.3 eV higher in energy near 1.0 $Å^{-1}$, where it is first visible, and converge on the calculation as $k_{\|}$ approaches $\bar{K}$. Also, it is difficult to see S_1 as it crosses E_F. Nearby, B_1 and B_2 may shift the apparent peak position. It is not uncommon to have a higher experimental value than the predicted value of the surface state energy; it could be as much as by 1 eV.[11] State S_1 shows the same shape of energy dispersion as the calculated surface state and both meet near the $\bar{K}$ point.

V. UNOCCUPIED ELECTRONIC STATES OF Ru ALONG THE $\bar{\Gamma}\,\bar{M}$ DIRECTION

The other high symmetry axis of the Ru(0001) surface is the $\bar{\Gamma}\,\bar{M}$ direction. IPE spectra were acquired along the $\bar{\Gamma}\,\bar{M}$ direction of the Ru(0001) surface at incident angles from 0° to 80° at 5° steps. Results using incident energies of 15.3 and 18.3 eV are presented in Figs. 6(a) and 6(b), respectively. At normal incidence, a main peak is observed at 0.7 eV and corresponds to the bulk state B_1 as was observed in Figs. 3 and 4. The IPE spectra in Fig. 6 do not have as many well-resolved features as did those from the $\bar{\Gamma}\,\bar{K}$ direction. There are some small changes in the intensity distribution between E_F and 2 eV, but they are not as prominent as those in the $\bar{\Gamma}\,\bar{K}$ direction, making it difficult to trace the peak dispersions from one spectrum to the next. The IPE spectra acquired at both incident energies, 15.3 and 18.3 eV, are similar in shape for a given $k_{\|}$. The IS at about 5 eV is barely seen in Fig. 6(b) at normal incidence.

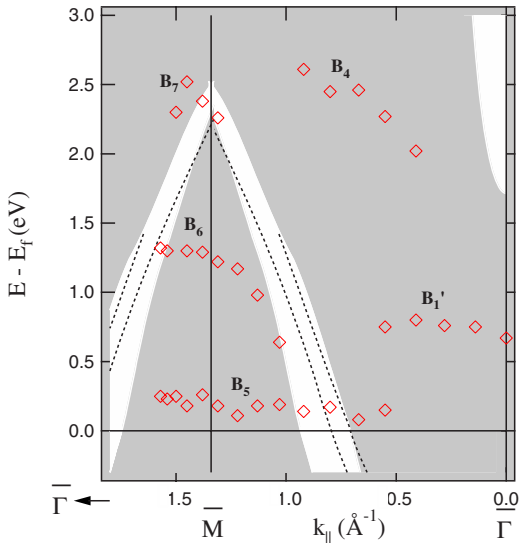

FIG. 9. (Color online) The energy dispersion of the enhanced features along the $\bar{\Gamma}\,\bar{M}$ direction of the Ru(0001) surface from Fig. 8(b).

In order to better observe the changes from one spectrum to the next, and thus follow the peak dispersions, we compare spectra from the Ru surface exposed to a small amount of CO (0.5 L) to spectra from the clean surface. The shapes of the spectra from the CO-exposed surface are relatively insensitive to the incident electron angle. As a result, difference spectra (i.e., $\Delta I = I_{\text{clean}} - I_{\text{CO/Ru}}$) accentuate the changes with angle in the clean spectra. To demonstrate this, Fig. 7 shows spectra from the $\bar{\Gamma}\,\bar{K}$ direction where this technique is applied. In Fig. 7(a), IPE spectra from the clean Ru(0001) surface (solid lines) and the CO-covered Ru surface (dotted lines) are normalized to the acquisition time and the current of the electron beam. The features in the spectra from the clean Ru(0001) surface are indicated, S_1, B_2, and B_3. The difference spectra ΔI are shown in Fig. 7(b), in which the features are indicated by tick marks and correspond to those features observed in Fig. 7(a). The features in Fig. 7(b) are sharper, more well resolved, and at the same energies as those features in Fig. 7(a).

To accentuate the features in the spectra along $\bar{\Gamma}\,\bar{M}$, we use the same technique. In Fig. 8(a), we show IPE spectra along the $\bar{\Gamma}\,\bar{M}$ direction with incident energy of 15.3 eV obtained from the clean and 0.5 L CO-exposed Ru(0001) surfaces. The IPE spectra are normalized by the current of the

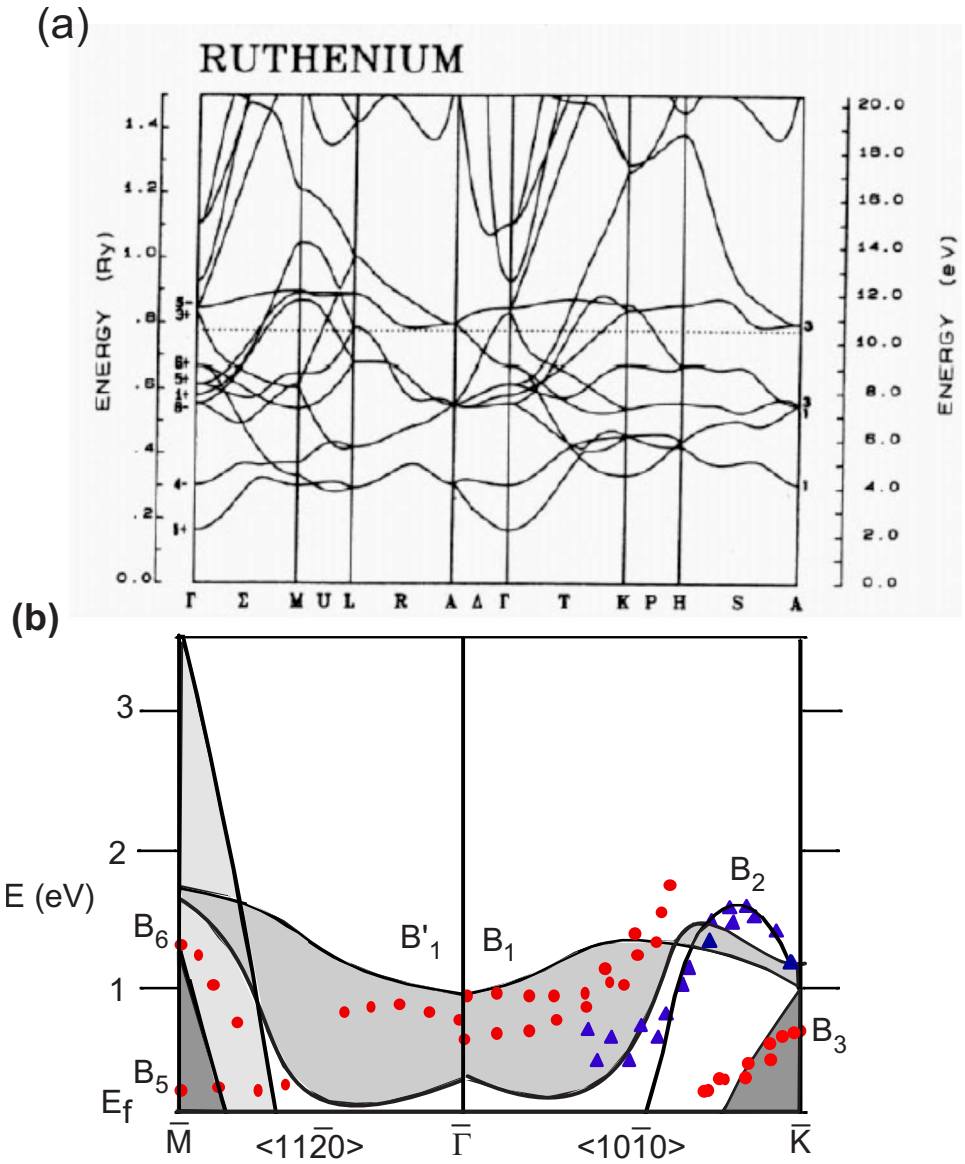

FIG. 10. (Color online) The electronic structure of Ru: (a) the bulk electronic structure of Ru along the high symmetry directions (after Ref. 7) and (b) the suggested bulk states of the electronic structure of Ru associated in the measured IPE spectra.

electron beam and the acquisition time. By subtracting the IPE intensity from the CO-covered Ru(0001) surface (dotted lines) from that of the clean Ru(0001) surface (solid lines) in Fig. 8(a), we generate the intensity difference spectra, $\Delta I = I_{\text{clean}} - I_{\text{CO/Ru}}$. These difference spectra are displayed in Fig. 8(b), where several features labeled as B_1', B_4, B_5, B_6, and B_7 are indicated by tick marks. It can now be seen that some of these peaks change energy as a function of angle, while others do not. The dispersions of the states with $k_\parallel$ are plotted in Fig. 9. As mentioned in the discussion of the data along the $\bar{\Gamma}\,\bar{K}$ direction, the slight difference between the spectra at 15.3 and 18.3 eV along the $\bar{\Gamma}\,\bar{M}$ direction is due to the incident electrons coupling to states of different $k_\parallel$ and decaying by direct transitions to final states of slightly different energy. At normal incidence, state B_1' is the same as state B_1, but now shows its dispersion along the $\bar{\Gamma}\,\bar{M}$ direction. As we see in Fig. 9, it has a flat dispersion with $k_\parallel$ from $\bar{\Gamma}$ to $k_\parallel = 0.6$ Å^{-1}. At larger $k_\parallel$, this state is no longer clearly visible. State B_4 shows an upward dispersion in the region of the projected bulk bands. State B_5 has a flat dispersion and follows the Fermi level from $k_\parallel = 0.5$ Å^{-1} to $\bar{M}$ and beyond. Note that the state crosses the projected band gap around $k_\parallel = 0.8$ Å^{-1}. State B_6 appears at $k_\parallel \sim 1.0$ Å^{-1} and disperses with $k_\parallel$ along the lower projected band edge for a short while and then bends to a flat dispersion at $\bar{M}$. Feature B_7 appears only for a very small range of $k_\parallel$ near $\bar{M}$, and the shape of its dispersion about $\bar{M}$ is similar to that of the band gap at $\bar{M}$. It is unclear whether there is significance to the observation that the state appears to lie within the projected band gap near $\bar{M}$. This might only be due to the narrow range of the gap. As a whole, all the states are in the projected bulk bands and thus are associated with bulk transitions. There are two predicted surface resonances along the $\bar{\Gamma}\,\bar{M}$ direction, as shown in Fig. 2 (Ref. 6) and Fig. 9. They cross the Fermi level at $k_\parallel = 0.7$ and 0.8 Å^{-1} and disperse to ~1.4 and ~2.3 eV above E_F, respectively. The surface resonances in the $\bar{\Gamma}\,\bar{M}$ direction are not observed. Recall that the predicted surface resonance along the $\bar{\Gamma}\,\bar{K}$ direction was also missing from our spectra. One possible reason is the weak interaction

between the incident electron and the surface resonance, whose wave function couples to bulk bands. The possibility of state B_6 or B_7 being the surface resonances in the $\bar{\Gamma}\,\bar{M}$ direction cannot be ruled out. Alternatively, the rapid dispersion of the surface resonance in the $\bar{\Gamma}\,\bar{M}$ direction may make it difficult to detect. If the surface resonance exists as predicted, a stronger signal and finer angular resolution would be needed to observe its rapid dispersion.

VI. COMPARISON WITH THE CALCULATED Ru BAND STRUCTURE

To make a direct comparison between our IPE results and the electronic states of Ru, the energy bands as a function of $k_\perp$ along the $\langle 0001\rangle$ direction are needed at a fixed value of $k_\parallel$ along the high symmetry directions. Then, if a possible direct transition from the higher unoccupied band coupling to a lower unoccupied band is found, the observed state can be compared with those predicted transitions.[4–7] However, other than along the ΓA, KH, and ML lines, detailed band structures along the $\langle 0001\rangle$ direction are not available in the literature. The next best approach is to compare the experimental results to the band structure of Ru along the high symmetry axes, as shown in Fig. 10(a). These results were calculated by Papaconstantopolous[7] using the augmented plane-wave method, including scalar-relativistic corrections within the local density approximation. The high symmetry axes of Ru in reciprocal space are shown in Fig. 1(b). The Fermi level in the figure is represented by a dotted line. In our IPES measurements, the interesting energy range of the states is a few eV above the Fermi level. Figure 10(b) shows the dispersion of selected bulk bands along the $\langle 10\bar{1}0\rangle$ ($\bar{\Gamma}\,\bar{K}$) and the $\langle 11\bar{2}0\rangle$ ($\bar{\Gamma}\,\bar{M}$) directions. The shaded areas are bounded by bands along the same direction in $k_\parallel$ that lie on the upper and lower faces of the bulk Brillouin zone. For example, the shaded areas in the $\bar{\Gamma}\,\bar{K}$ direction are bounded by the bands along the ΓK and the AH directions. Similarly, for the $\bar{\Gamma}\,\bar{M}$ direction, the shaded regions are bounded by bands along the ΓM and AL directions. The dispersions of the observed features in the IPE spectra along the $\bar{\Gamma}\,\bar{K}$ (Fig. 5) and the $\bar{\Gamma}\,\bar{M}$ (Fig. 9) directions are displayed in Fig. 10(b).

Even though the dispersions in those directions are not exactly the same, the shape and the energy range of the bulk band dispersions in the $\langle 10\bar{1}0\rangle$ and $\langle 11\bar{2}0\rangle$ directions serve as a reference to which the observed unoccupied states in Ru(0001) surface can be compared. From the dispersions of the features in the Ru(0001) surface along the $\bar{\Gamma}\,\bar{K}$ and the $\bar{\Gamma}\,\bar{M}$ directions, the bulk bands that most closely correspond to the observed features, B_1, B_1', B_2, B_3, B_5, and B_6, are suggested in Fig. 10(b). These bands were chosen owing to their shape and the position as compared to the observed dispersions in those directions. It is noted that not every observed feature (for example, B_4 and B_7) could be associated with a corresponding bulk band in Fig. 10(a). This is because the experimental results probe all bands that project into the Ru(0001) surface, while the results in Fig. 10(a) report only bulk bands along high symmetry axes.

In Fig. 10(b), band B_1 of Ru is a d-band derived state, which has a flat dispersion with $k_\parallel$ in both directions. This character is observed as in the experiment. Bands B_2 and B_3 disperse in the $\langle 10\bar{1}0\rangle$ direction and are very well described by the bands along the high symmetry ΓK line of the bulk Brillouin zone. State B_6 disperses along the $\langle 11\bar{2}0\rangle$ direction, ending at $\bar{M}$ at about 1.3 eV. The rapid dispersion of this state suggests that it is of sp-band character. State B_5 has a very flat dispersion along the $\langle 11\bar{2}0\rangle$ direction and is difficult to associate with any bulk band. Even though the absence of a complete set of theoretical data prevents a direct comparison between the observed features and the bulk band structure, the overall behavior of the observed features can be well understood in terms of the general properties of bulk band dispersions.

VII. CONCLUSIONS

IPE spectra of clean Ru(0001) were measured along the $\bar{\Gamma}\,\bar{K}$ and the $\bar{\Gamma}\,\bar{M}$ high symmetry axes of the SBZ. In the $\bar{\Gamma}\,\bar{K}$ direction, the IPE spectra show features interpreted as direct transitions between unoccupied Ru bulk states. The dispersions of these features overlap the Ru(0001) projected band structure. A surface state is observed from $k_\parallel = 1.1$ Å^{-1} at 0.7 eV to $k_\parallel = 1.5$ Å^{-1} at 1 eV along the $\bar{\Gamma}\,\bar{K}$ direction and agrees with the calculation by Holzwarth and Chelikowsky.[6] The intensity of the surface state is weak compared to strong bulk transitions, making the study of its behavior difficult. Detailed features of the clean Ru(0001) surface could be obtained by subtracting the IPE spectra intensity of CO-covered Ru(0001) surface from that of the clean surface. For example, the surface state on a clean Ru(0001) surface is clearly observed in the subtracted IPE spectra.

In the $\bar{\Gamma}\,\bar{M}$ direction, bulk direct transitions are observed, but the calculated surface resonance is not observed in our IPE results. The bulk direct transitions are compared to the calculated band structure of the bulk states by Papaconstantopolous.[7] We found that the dispersion of the observed spectral features is well described by several bulk bands in the calculation.

ACKNOWLEDGMENT

The authors wish to thank H. Nozoye for use of the Ru(0001) crystal in these experiments.

*Present address: Telcordia Technologies, Inc., One Telcordia Drive, Piscataway, NJ 08854-4182.

[1] D. W. Goodman, R. D. Kelley, T. E. Madey, and J. T. Yates, J. Catal. **63**, 226 (1980).
[2] D. W. Goodman and J. M. White, Surf. Sci. **90**, 201 (1979).
[3] B. A. Sexton and G. A. Somorjai, J. Catal. **46**, 167 (1977).
[4] J. R. Chelikowsky, C. T. Chan, and S. G. Louie, Phys. Rev. B **34**, 6656 (1986).
[5] P. J. Feibelman, Phys. Rev. B **26**, 5347 (1982).
[6] N. A. W. Holzwarth and J. R. Chelikowsky, Solid State Commun. **53**, 171 (1985).
[7] D. A. Papaconstantopolous, *Handbook of the Band Structure of Elemental Solids* (Plenum, New York, 1986).
[8] F. J. Himpsel, K. Christmann, P. Heimann, and D. E. Eastman, Phys. Rev. B **23**, 2548 (1981).
[9] M. Lindroos, P. Hofmann, and D. Menzel, Phys. Rev. B **33**, 6798 (1986).
[10] M. Lindroos, H. Pfnür, and D. Menzel, Phys. Rev. B **33**, 6684 (1986).
[11] T. Pelzer, G. Ceballos, F. Zbikowski, B. Willerding, K. Wandelt, U. Thomann, C. Reuss, T. Fauster, and J. Braun, J. Phys.: Condens. Matter **12**, 2193 (2000).
[12] J. C. Fuggle, T. E. Madey, M. Steinkilberg, and D. Menzel, Surf. Sci. **52**, 521 (1975).
[13] B. Hammer, Y. Morikawa, and J. K. Norskov, Phys. Rev. Lett. **76**, 2141 (1996).
[14] D. Heskett and E. W. Plummer, Surf. Sci. **164**, 490 (1985).
[15] T. E. Madey, Surf. Sci. **79**, 575 (1979).
[16] T. E. Madey and D. Menzel, Jpn. J. Appl. Phys., Suppl. **2**, 229 (1974).
[17] R. Persaud and R. H. Prince, Surf. Sci. **282**, 91 (1993).
[18] J. Rogozik and V. Dose, Surf. Sci. **176**, L847 (1986).
[19] E. D. Williams and W. H. Weinberg, Surf. Sci. **82**, 93 (1979).
[20] M. Stichler, C. Keller, C. Heske, M. Staufer, U. Birkenheuer, N. Rosch, W. Wurth, and D. Menzel, Surf. Sci. **448**, 164 (2000).
[21] M. Stichler and D. Menzel, Surf. Sci. **391**, 47 (1997).
[22] E. Umbach, S. Kulkarni, P. Feulnaer, and D. Menzel, Surf. Sci. **88**, 65 (1979).
[23] M. Y. Chou and J. R. Chelikowsky, Phys. Rev. Lett. **59**, 1737 (1987).
[24] M. Y. Chou and J. R. Chelikowsky, Phys. Rev. B **39**, 5623 (1989).
[25] P. Hofmann and D. Menzel, Surf. Sci. **152/153**, 382 (1985).
[26] K. L. Kostov, H. Rauscher, and D. Menzel, Surf. Sci. **278**, 62 (1992).
[27] J. Landskron, W. Moritz, B. Narloch, G. Held, and D. Menzel, Surf. Sci. **441**, 91 (1999).
[28] D. Menzel, H. Pfnur, and P. Feulner, Surf. Sci. **126**, 374 (1983).
[29] B. Narloch, G. Held, and D. Menzel, Surf. Sci. **340**, 159 (1995).
[30] A. Schiffer, P. Jakob, and D. Menzel, Surf. Sci. **389**, 116 (1997).
[31] J. C. Fuggle, M. Steinkilberg, and D. Menzel, Chem. Phys. **11**, 307 (1975).
[32] H. Over, H. Bludau, R. Kose, and G. Ertl, Phys. Rev. B **51**, 4661 (1995).
[33] J. A. Rodriguez and D. W. Goodman, Science **257**, 897 (1992).
[34] S. Schwegmann, H. Over, V. DeRenzi, and G. Ertl, Surf. Sci. **375**, 91 (1997).
[35] D. Heskett, E. W. Plummer, R. A. de Paola, and W. Eberhardt, Phys. Rev. B **33**, 5171 (1986).
[36] K. Jacobi, H. Shi, H. Dietrich, and G. Ertl, Surf. Sci. **333**, 69 (1995).
[37] H. Kondoh and H. Nozoye, J. Phys. Chem. **98**, 390 (1994).
[38] H. Kondoh, H. Orita, and H. Nozoye, J. Phys. Chem. **99**, 8790 (1995).
[39] P. J. Feibelman, Phys. Rev. B **67**, 035420 (2003).
[40] S. R. Puisto, T. J. Lerotholi, G. Held, and D. Menzel, Surf. Rev. Lett. **10**, 487 (2003).
[41] P. J. Feibelman, Science **295**, 99 (2002).
[42] S. Meng, L. F. Xu, E. G. Wang, and S. Gao, Phys. Rev. Lett. **89**, 176104 (2002).
[43] S. Meng, S.-Y. Yang, and E.-G. Wang, Wuli Huaxue Xuebao **32**, 219 (2003).
[44] S. Meng, E. G. Wang, and S. Gao, Phys. Rev. B **69**, 195404 (2004).
[45] J. Weissenrieder, A. Mikkelsen, J. N. Andersen, P. J. Feibelman, and G. Held, Phys. Rev. Lett. **93**, 196102 (2004).
[46] K. Andersson, A. Nikitin, L. G. M. Pettersson, A. Nilsson, and H. Ogasawara, Phys. Rev. Lett. **93**, 196101 (2004).
[47] C. Benndrof, E. Bertel, V. Dose, W. Jacob, N. Memmel, and J. Rogozik, Surf. Sci. **191**, 455 (1987).
[48] D. A. Arena, F. G. Curti, and R. A. Bartynski, Surf. Sci. **369**, 117 (1996).
[49] F. G. Curti, A. Danese, and R. A. Bartynski, Phys. Rev. Lett. **80**, 2213 (1998).
[50] M. Grunze, H. Ruppender, and O. Elshazly, J. Vac. Sci. Technol. A **6**, 1266 (1988).
[51] K. Wandelt, J. Hulse, and J. Kuppers, Surf. Sci. **104**, 212 (1981).